Available online at www.sciencedirect.com
SCIENCE DIRECT®
PERGAMON
International Journal of Heat and Mass Transfer 46 (2003) 4877–4883
International Journal of HEAT and MASS TRANSFER
www.elsevier.com/locate/ijhmt

Characteristics and correlations of VOC emissions from building materials

Yinping Zhang *, Ying Xu

Department of Building Science, Tsinghua University, Beijing 100084, PR China

Received 2 January 2003; received in revised form 25 March 2003

Abstract

An improved mass transfer model which considers the air–material mass transfer resistance was used to analyze volatile organic compound (VOC) emissions from building materials. The results showed that the dimensionless emission rate of VOCs is only a function of the ratio of mass transfer Biot number to the partition coefficient and of mass transfer Fourier number. These two parameters were used to fit experimental data for empirical correlations of VOC emission data. Numerical results, which agreed well with the experiment data, were used to develop several correlations describing the VOC emission characteristics from building materials.

Keywords: Volatile organic compounds; Mass diffusion; Indoor air quality; Building material

1. Introduction

Indoor air quality problems due to the emissions of volatile organic compounds (VOCs) from building materials may cause various symptoms, such as headaches; eye, nose, or throat irritations; dry coughs; dizziness and nausea; difficulty in concentrating and tiredness [1–4]. Since building materials are important sources of VOCs in indoor environments, their emission characteristics should be studied.

The characteristics of VOC sources and sinks have been studied experimentally, analytically and numerically. Although experimental methods provide the most realistic results, experiments require expensive, well-controlled facilities. In addition, results for specified test conditions may not be directly applicable for other conditions [4]. Therefore, many researchers have stressed the importance of simulating VOC emissions from building materials.

Generally speaking, there are two kinds of VOC emission models in the literature [4,5]. The first type is the so-called empirical model, which is based solely on statistical analysis of emission data obtained from environment chamber testing. Typical examples are the first-order decay model and the power-law decay model [6]. Although empirical models are simple and easy to use, they are not able to provide insight into the physical emission mechanisms and can not be easily scaled from the test conditions to building conditions. The second type of models is based on mass transfer theory and is thus called mass transfer models. Unlike the empirical models, mass transfer models can predict the VOC emissions for various conditions for known physical parameters. Dunn et al. [7], Clausen et al. [8], and Little et al. [9] neglected the mass transfer resistance through the air phase boundary layer to obtain analytical solutions. Yang et al. [10] developed a numerical model to simulate dry material emission processes which considered both the boundary layer resistance and the internal resistance, but the solution was very time consuming. Xu and Zhang [11] expanded on the work of Little et al. [9] by including the mass transfer resistance through the air phase boundary layer.

The objective of this paper is to analyze the general characteristics of VOC emissions from building materials to develop simulation based correlations describing the emission characteristics.

* Corresponding author. Tel.: +86-10-6277-2518; fax: +86-10-6277-3461.
E-mail address: zhangyp@mail.tsinghua.edu.cn (Y. Zhang).

0017-9310/$ - see front matter © 2003 Elsevier Ltd. All rights reserved.
doi:10.1016/S0017-9310(03)00352-1

Nomenclature

A	building material emission surface area (m^2)
ACH	air change rate
Bi_m	mass transfer Biot number, $Bi_m = h_m L/D$ (dimensionless)
C	VOC concentration in building material ($mg\,m^{-3}$)
C_0	initial VOC concentration in building material ($mg\,m^{-3}$)
$C_s(t)$	VOC concentration in air adjacent to the interface ($mg\,m^{-3}$)
$C_\infty(t)$	VOC concentration in atmosphere or in chamber ($mg\,m^{-3}$)
C^*	dimensionless concentration, $C^* = (C - KC_\infty)/(C_0 - KC_\infty)$
D	mass diffusion coefficient for compound in building material ($m^2\,s^{-1}$)
ε_1	relative error in calculating $\dot{m}(t)$
ε_2	relative error in calculating $m(t)$
Fo_m	mass transfer Fourier number, $Fo_m = Dt/L^2$ (dimensionless)
h_m	convective mass transfer coefficient ($m\,s^{-1}$)
K	partition coefficient between building material and air (dimensionless)
L	building material slab thickness (m)
M	total VOC emissions per unit area building material ($mg\,m^{-2}$)
$m(t)$	total VOC emissions per unit area building material before time t ($mg\,m^{-2}$)
$\dot{m}(t)$	VOC emission rate per unit area building material at time t ($mg\,m^{-2}\,s^{-1}$)
$m^*(t)$	$m(t)/M$ (dimensionless)
$\dot{m}^*$	dm^*/dFo_m (dimensionless)
PB	particle board
Q	volumetric air flow rate through chamber ($m^3\,s^{-1}$)
t	time (s)
TVOC	total volatile organic compounds
V	air volume in chamber (m^3)
VOC	volatile organic compound
x	linear distance (m)
X	dimensionless linear distance, $X = x/L$

Subscript

c	critical value

2. VOC mass transfer

The mass transfer model assumes that the VOCs are emitted from a single uniform layer of material with a VOC impermeable backing material. A schematic of the idealized building material slab in air is shown in Fig. 1. The governing equation describing the transient diffusion through the slab is

$$\frac{\partial C(x,t)}{\partial t} = D\frac{\partial^2 C(x,t)}{\partial x^2}, \tag{1}$$

where $C(x,t)$ is the VOC concentration in the building material slab. The initial condition assumes that the VOC is uniformly distributed throughout the building material slab, i.e.,

$$C(x,t) = C_0 \quad \text{for } 0 \leqslant x \leqslant L, \;\; t = 0. \tag{2}$$

Since the slab is resting on a VOC impermeable surface, the boundary condition at the lower slab surface is

$$\frac{\partial C(x,t)}{\partial t} = 0, \quad t > 0, \;\; x = 0. \tag{3}$$

A boundary condition of the third kind is imposed on the upper slab surface (Fig. 1):

$$-D\frac{\partial C(x,t)}{\partial x} = h_m(C_s(t) - C_\infty(t)), \quad t > 0, \;\; x = 0. \tag{4}$$

Almost all of the physically based models in the literature assumed that $C_s(t) = C_\infty(t)$, which means that h_m is infinite [7–9] which is a special case of Eq. (4).

In addition, equilibrium exists on the air–material interface [9].

$$C(x,t) = KC_s(t), \quad t > 0, \;\; x = L, \tag{5}$$

where K is the partition coefficient.

Eqs. (1)–(5) were solved using separation of variables:

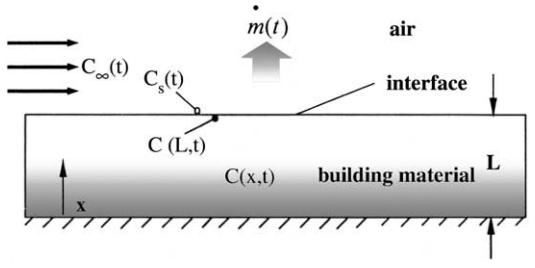

Fig. 1. Schematic of building material slab emissions geometry.

$$C(x,t) = KC_\infty(t) + \sum_{m=1}^{\infty} \frac{\sin(\beta_m L)}{\beta_m} \cdot \frac{2(\beta_m^2 + H^2)}{L(\beta_m^2 + H^2) + H} \cdot \cos(\beta_m x) \cdot \left[(C_0 - KC_\infty(0))\mathrm{e}^{-D\beta_m^2 t} + \int_0^t \mathrm{e}^{-D\beta_m^2(t-\tau)} \cdot K\,\mathrm{d}C_\infty(\tau) \right], \quad (6)$$

where $H = h_m/KD$ and β_m ($m = 1, 2, \ldots$) are the positive roots of

$$\beta_m \cdot \tan(\beta_m L) = H. \quad (7)$$

Eq. (6) gives the VOC concentration in the building material slab as a function of time and the distance from the slab base.

Thus, the VOC emission rate per unit area at time t, $\dot{m}(t)$, and the total VOC emissions, $m(t)$, emitted per unit area of building material slab until time t are

$$\dot{m}(t) = -D \cdot \left.\frac{\partial C(x,t)}{\partial x}\right|_{x=L} = D \cdot \sum_{m=1}^{\infty} \sin^2(\beta_m L) \cdot \frac{2(\beta_m^2 + H^2)}{L(\beta_m^2 + H^2) + H} \cdot \left[(C_0 - KC_\infty(0))\mathrm{e}^{-D\beta_m^2 t} + \int_0^t \mathrm{e}^{-D\beta_m^2(t-\tau)} \cdot K\,\mathrm{d}C_\infty(\tau) \right], \quad (8)$$

$$m(t) = -\int_0^t D \cdot \left.\frac{\partial C(x,t)}{\partial x}\right|_{x=L} \mathrm{d}t = D \int_0^t \sum_{m=1}^{\infty} \sin^2(\beta_m L) \cdot \frac{2(\beta_m^2 + H^2)}{L(\beta_m^2 + H^2) + H} \cdot \left[(C_0 - KC_\infty(0))\mathrm{e}^{-D\beta_m^2 t} + \int_0^t \mathrm{e}^{-D\beta_m^2(t-\tau)} \cdot K\,\mathrm{d}C_\infty(\tau) \right] \mathrm{d}t. \quad (9)$$

3. Comparison of predictions

The one-dimensional model, was verified by comparing the predicted instantaneous VOC concentrations for a flat slab in a small environmental chamber to experimental data [4]. A schematic of the experimental setup is given in Fig. 2 and the experimental conditions are listed in Table 1. The properties used in the model, the diffusion coefficient, D; the partition coefficient, K; the initial concentration, C_0 and the convective mass transfer coefficient, h_m were obtained by Yang et al. [10] through a detailed numerical study of the experimental data.

The VOC concentration in the chamber is given by

$$\frac{\mathrm{d}C_\infty(t)}{\mathrm{d}t} \cdot V = A \cdot \dot{m}(t) - Q \cdot C_\infty(t). \quad (10)$$

Eqs. (9) and (10) can be combined to give the instantaneous VOC concentration in the chamber air. The predictions are compared with those of Little's model and the experimental data in Fig. 3. The data shows that the results from the model agree well with the experimental results. However, Little's model tends to initially significantly overestimate the VOC concentration in the air because Little's model neglects the convective mass transfer resistance. Initially, the VOC concentration

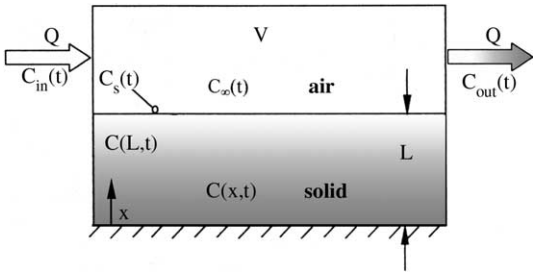

Fig. 2. Schematic of simplified environmental chamber.

Table 1
Experimental conditions (Panel A) and parameters for the building material slabs (Panel B)

Panel A			
Temperature (°C)	23 ± 0.5		
Relative humidity (%)	50 ± 0.5		
Air change rate (h^{-1})	1 ± 0.05		
Chamber volume (m × m × m)	$0.5 \times 0.4 \times 0.25$		
Building material slab size (m × m × m)	$0.212 \times 0.212 \times 0.0159$		
Panel B			
VOC	TVOC	TVOC	Hexanal
Particle boards	PB 1	PB 2	PB 2
Mass diffusion coefficient, D (1×10^{11} m^2 s^{-1})	7.65	7.65	7.65
Initial concentration, C_0 (1×10^{-7} μg m^{-3})	5.28	9.86	2.96
Partition coefficient, K	3289	3289	3289

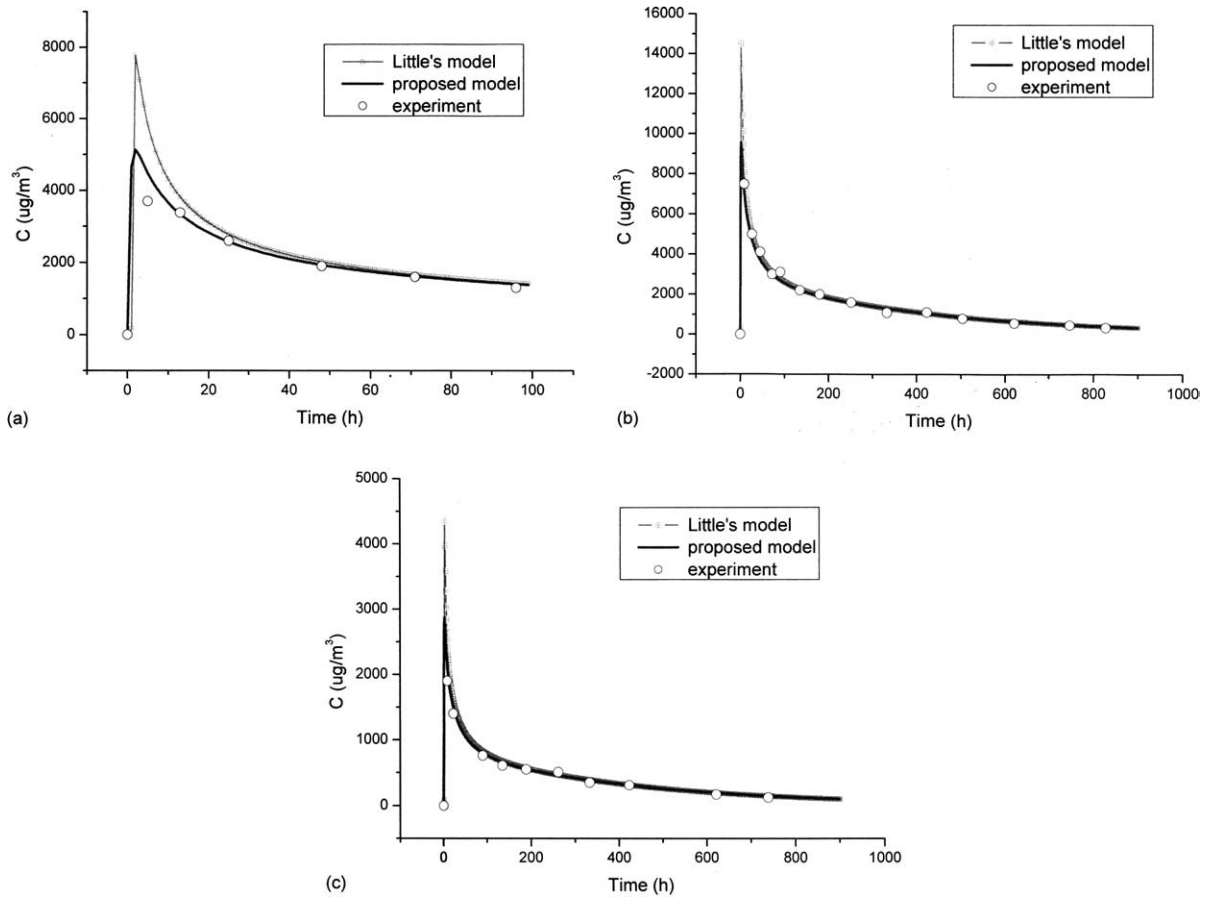

Fig. 3. Comparison of model and experimental results for instantaneous volatile concentrations: (a) TVOC, PB 1; (b) TVOC, PB 2; (c) Hexanal, PB 2.

near the surface in the material is relatively high, so neglecting the convective mass transfer resistance results in a large amount of mass transfer in the air. Later, the volatile concentration near the surface has decreased so that the internal mass diffusion resistance is much more important than the convective resistance so the errors caused by neglecting the convective resistance become very small.

4. VOC emission correlations

4.1. Dimensionless equations

The general characteristics of VOC emissions from building materials were predicted by introducing the following variables into Eqs. (1)–(5):

$$Fo_{\mathrm{m}} = \frac{Dt}{L^2} \quad \text{and} \quad Bi_{\mathrm{m}} = \frac{h_{\mathrm{m}} \cdot L}{D}, \tag{11}$$

where Fo_{m} is the mass transfer Fourier number (dimensionless time) and Bi_{m} is the mass transfer Biot number. The dimensionless concentration and distance are then

$$C^* = \frac{C - KC_\infty}{C_0 - KC_\infty} \quad \text{and} \quad X = \frac{x}{L}. \tag{12}$$

Rearranging Eqs. (1)–(5) yields the following dimensionless equations:

$$\frac{\partial C^*}{\partial Fo_{\mathrm{m}}} = \frac{\partial^2 C^*}{\partial X^2}, \quad 0 < X < 1, \ Fo_{\mathrm{m}} > 0, \tag{13.1}$$

$$C^* = 1, \quad 0 \leqslant X \leqslant 1, \ Fo_{\mathrm{m}} = 0, \tag{13.2}$$

$$\frac{\partial C^*}{\partial X} = 0, \quad X = 0, \ Fo_{\mathrm{m}} > 0, \tag{13.3}$$

$$\frac{\partial C^*}{\partial X} = -\frac{Bi_{\mathrm{m}}}{K} C^*, \quad X = 1, \ Fo_{\mathrm{m}} > 0. \tag{13.4}$$

The solutions of these equations are

$$C^* = 2 \sum_{n=1}^{\infty} \mathrm{e}^{-u_n^2 Fo_{\mathrm{m}}} \frac{\sin u_n \cos(u_n X)}{u_n + \sin u_n \cos u_n}, \tag{14}$$

$$m^* = \frac{m(t)}{M} = \sum_{m=1}^{\infty} \frac{2\sin^2 u_n}{u_n^2 + u_n \sin u_n \cos u_n}(1 - e^{-u_n^2 Fo_m}), \quad (15)$$

$$\dot{m}^* = \frac{dm^*}{dFo_m} = \sum_{m=1}^{\infty} \frac{2u_n^2 \cdot \sin^2 u_n}{u_n^2 + u_n \sin u_n \cos u_n} \cdot e^{-u_n^2 Fo_m}, \quad (16)$$

where u_n are the positive roots of

$$u_n tg u_n = Bi_m/K \quad (n = 1, 2, \ldots). \quad (17)$$

4.2. General characteristics of VOC emissions

From Eqs. (14)–(16), it is seen that the dimensionless concentration C^*, dimensionless total emissions m^* and dimensionless emission rate $\dot{m}^*$ are functions of

$$C^* = f_1\left(\frac{Bi_m}{K}, Fo_m, X\right), \quad (18)$$

$$m^* = f_2\left(\frac{Bi_m}{K}, Fo_m\right), \quad (19)$$

$$\dot{m}^* = f_3\left(\frac{Bi_m}{K}, Fo_m\right). \quad (20)$$

Eqs. (18)–(20) illustrate the functional relationships between the dependent and independent variables. The equations show that C_0 does not influence C^*, m^* or $\dot{m}^*$ and that although m^* and $\dot{m}^*$ depend on the building material properties, D and K; the mass convective coefficient, h_m; the slab thickness L and time, the dependence may be described by grouping these variables as Bi_m/K and Fo_m. Therefore, the VOC emission rates can be represented by two dimensionless groups instead of the original five parameters. Moreover, once the form of the functional dependence of Eqs. (19) and (20) has been obtained for a particular surface geometry, e.g. from laboratory measurements, it is known for all such similar geometries for various contaminants, building materials, air flow velocities, and slab thicknesses, as long as the range of the dimensionless parameters are similar. Therefore, Eqs. (19) and (20) will be used to summarize the general characteristics of VOC emissions from building materials.

4.3. VOC emission correlations

A literature review has shown that for most building materials in indoor environments, Bi_m/K is in the range of 20–700. For example, Table 2 lists the values of Bi_m/K for VOC emissions from indoor materials studied by Little et al. [9]. The Bi_m/K range for these materials are all $20 \leqslant Bi_m/K \leqslant 700$. Bi_m/K values for dry building materials in practical applications are also in this range.

Numerical results from the model for this range were fitted using a least square analysis to determine the functional relationship for the dimensionless emissions in Eq. (19) for small Fo_m:

$$m^* = 1.22 \cdot (Bi_m/K)^{9.70\times10^{-3}} \cdot Fo_m^{0.601}, \quad 0 \leqslant Fo_m < 0.3. \quad (21)$$

The correlation factor for the data, R^2, was 0.992. The standard deviation between the correlation and the numerical data was 0.0126. For larger Fo_m,

$$m^* = 1.12 \cdot (Bi_m/K)^{-1.75\times10^{-3}} \cdot e^{-0.191/Fo_m}, \quad 0.3 \leqslant Fo_m < 2. \quad (22)$$

The correlation factor was 0.996 and the standard deviation between the correlation and the numerical data was 0.00760. For larger Fo_m,

$$m^* = 1, \quad Fo_m \geqslant 2. \quad (23)$$

The numerical results for $Fo_m = 2$ predicted $m^* = 0.99$ with m^* increasing with increasing Fo_m and approaching 1 as Fo_m approaches infinity. Thus, $Fo_m = 2$ can be taken as the time for complete emission of the volatiles from the building material.

Table 2
Bi_m/K for VOC emissions from common indoor materials [9]

VOCs	D (1×10^{12} m^2 s^{-1})	K	L (mm)	h_m (m h^{-1})	Bi_m/K
Styrene	4.1	4200	1.25	1.57	31.7
				4.2	84.7
Ethylenzene and xylenes	4.3	2400	1.25	1.57	52.8
				4.2	141.3
Formaldehyde	3.2	11,000	2.0	1.57	24.8
				4.2	66.3
2,2,4-Trimethylpentane	0.06	59,000	2.0	1.57	246.4
				4.2	659.1
1,2-Propanediol	0.07	180,000	2.0	1.57	122.2
				4.2	326.8
4-Ethenyl-cyclohexene	2.1	1700	1	1.57	122.2
				4.2	326.8

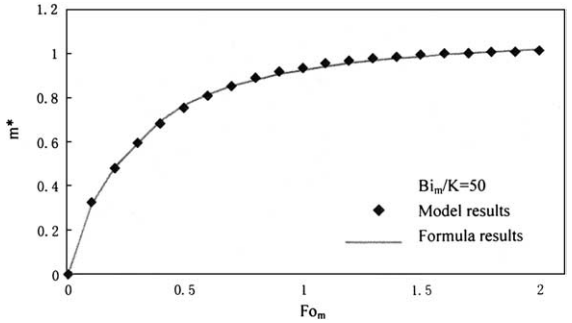

Fig. 4. Variation of m^* with Bi_m/K and Fo_m ($Bi_m/K = 50$, $0 \leqslant Fo_m \leqslant 2$).

Fig. 4 shows the relationship between m^* and Fo_m for $Bi_m/K = 50$. Fig. 5 compares the predictions from the correlations and the model for $Bi_m/K = 50$.

Similarly, for Bi_m/K in the range 20–700, a least square fit of the numerical results from the model gives the following correlations for the dimensionless emission rate corresponding to Eq. (20):

$$\dot{m}^* = 9.73 \cdot (Bi_m/K)^{2.32\times10^{-2}} \cdot e^{-73.6 Fo_m}, \quad 0 \leqslant Fo_m < 0.01. \tag{24}$$

The correlation factor was 0.98 and the standard deviation was 0.34. For larger Fo_m, the correlation is

$$\dot{m}^* = 0.551 \cdot (Bi_m/K)^{1.90\times10^{-3}} \cdot Fo_m^{-0.504}, \quad 0.01 \leqslant Fo_m < 0.2. \tag{25}$$

The correlation factor was 0.998 and the standard deviation was 0.024.

$$\dot{m}^* = 3.56 \cdot (Bi_m/K)^{-0.101} \cdot e^{-2.44 Fo_m}, \quad 0.2 \leqslant Fo_m < 5. \tag{26}$$

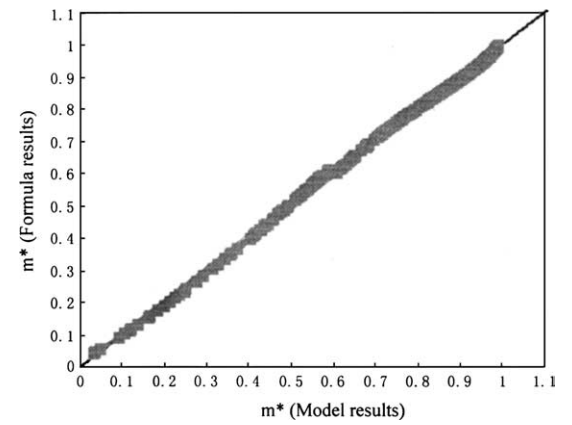

Fig. 5. Comparison of correlation and model results for total emissions for $Bi_m/K = 50$.

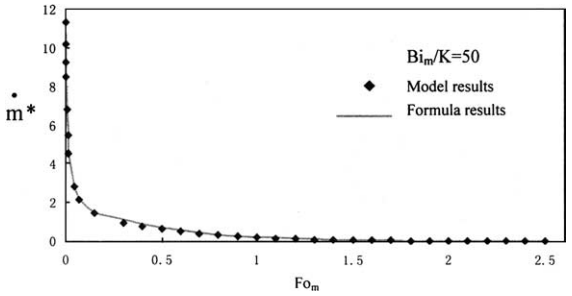

Fig. 6. Variation of $\dot{m}^*$ with Bi_m/K and Fo_m ($Bi_m/K = 50$, $0 \leqslant Fo_m \leqslant 2.5$).

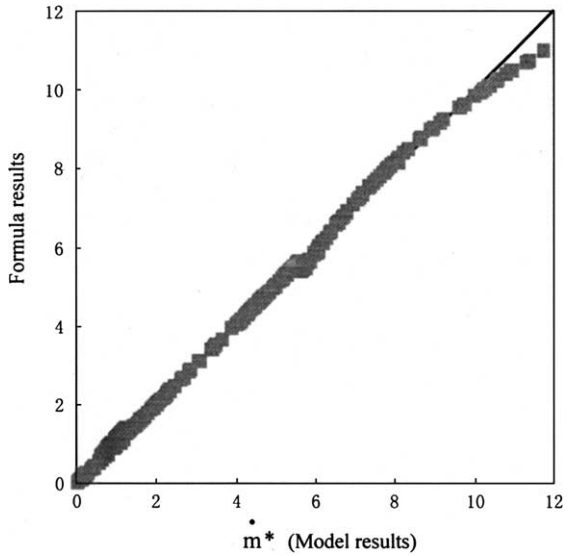

Fig. 7. Comparison of correlation and model results for emissions rate for $Bi_m/K = 50$.

The correlation factor was 0.9995 and the standard deviation was 0.025. For large Fo_m,

$$\dot{m}^* = 0, \quad Fo_m > 5. \tag{27}$$

Fig. 6 shows the relationship between $\dot{m}^*$ and Fo_m for $Bi_m/K = 50$. Fig. 7 compares the predictions from the correlations and the model for $Bi_m/K = 50$.

5. Conclusions

(1) A mass transfer model including the convective mass transfer resistance through the air phase boundary layer was used to precisely predict the emissions of VOCs from indoor material for a range of conditions.
(2) Although the dimensionless total emissions, m^* and the dimensionless emission rate, $\dot{m}^*$ depend on the building material properties, D and K; the convec-

tive mass transfer coefficient, h_m; the slab thickness, L and the time, the dependence may be more generally described by grouping these variables as Bi_m/K and Fo_m. These dimensionless variables were used to formulate empirical correlations for VOC emissions from building materials. Once the form of the functional dependence of Eqs. (19) and (20) has been obtained for a particular surface geometry for specific conditions, the correlation may be applied to different contaminants, building materials, air flow velocities, and slab thicknesses, as long as the dimensionless parameters are the same.

(3) For constant VOC background concentration C_∞, Eqs. (21)–(23) can predict the values of $\dot{m}(t)$ and $m(t)$.

Acknowledgements

This work was supported by National Nature Science Foundation of China (Project no. 50276033) and by Tsinghua University (Project no. 200007005).

References

[1] Y.M. Kim, S. Harrad, R.M. Harrison, Concentrations and sources of VOCs in urban domestic and public microenvironments, Environ. Sci. Technol. 35 (2001) 997–1004.

[2] R. Meininghaus, T. Salthammer, Interaction of volatile organic compounds with indoor materials—a small-scale screening method, Atmos. Environ. 33 (1999) 2395–2401.

[3] L. Molhave, The sick buildings and other buildings with indoor climate problems, Environment 15 (1) (1989) 65–74.

[4] X. Yang, Study of Building Materials Emissions and Indoor Air Quality, PhD Dissertation, Massachusetts Institute of Technology, Cambridge, MA, 1999.

[5] R. Merrill, R. Steiber, L. Nelms, Screening methods for the identification of organic emissions from indoor air pollution sources, Atmos. Environ. 21 (2) (1987) 331–336.

[6] J.P. Zhu, J.S. Zhang, C.Y. Shaw, Comparison of models for describing measured VOC emissions from wood-based panels under dynamic chamber test condition, Chemosphere 44 (2001) 1253–1257.

[7] J.E. Dunn, Models and statistical methods for gaseous emission testing of finite source in well-mixed chambers, Atmos. Environ. 21 (2) (1987) 425–430.

[8] P.A. Clausen, P. Wolkoff, E. Holst, P.A. Nielsen, Long-term emission of volatile organic compounds from water-borne paints—methods of comparison, Indoor Air 4 (1991) 562–576.

[9] J.C. Little, A.T. Hodgson, A.J. Gadgil, Modeling emissions of volatile organic compounds from new carpets, Atmos. Environ. 28 (2) (1994) 227–234.

[10] X. Yang, Q. Chen, J.S. Zhang, R. Magee, J. Zeng, C.Y. Shaw, Numerical simulation of VOC emissions from dry materials, Build. Environ. 36 (10) (2001) 1099–1107.

[11] Y. Xu, Y.P. Zhang, An improved mass transfer based model for analyzing VOC emissions from building materials, Atmos. Environ. 37 (2003) 2497–2505.